

# Electronic Supplementary Information

## Co-ligand tuning of MOF structural anisotropy for giant optical birefringence

Svyatoslav A. Povarov\*<sup>a</sup>, Ekaterina D. Iukhnevich<sup>a,b</sup>, Pavel V. Alekseevskiy<sup>a,b</sup>,  
Dmitry I. Pavlov<sup>c</sup>, Andrei S. Potapov<sup>c</sup>, Irina D. Yushina<sup>d</sup>, Valentin A. Milichko<sup>b,e</sup>,  
Alena N. Kulakova\*<sup>b</sup>

<sup>a</sup> Qingdao Innovation and Development Center, Harbin Engineering University, Qingdao, Shandong, 266000 China e-mail: [s.povarov@metalab.ifmo.ru](mailto:s.povarov@metalab.ifmo.ru).

<sup>b</sup> School of Physics and Engineering, ITMO University, St. Petersburg 197101, Russia; e-mail: [alengkulakova@gmail.com](mailto:alengkulakova@gmail.com).

<sup>c</sup> Nikolaev Institute of Inorganic Chemistry, Siberian Branch of the Russian Academy of Sciences, Novosibirsk 630090, Russia.

<sup>d</sup> South Ural State University, 454080, Chelyabinsk, Russia.

<sup>e</sup> Université de Lorraine, Institut Jean Lamour, Nancy, 54000, France

\*Corresponding authors' e-mails: [s.povarov@metalab.ifmo.ru](mailto:s.povarov@metalab.ifmo.ru),  
[alena.kulakova@metalab.ifmo.ru](mailto:alena.kulakova@metalab.ifmo.ru)

## Experimental section

### Materials

$\text{Cd}(\text{NO}_3)_2 \cdot 4\text{H}_2\text{O}$  (98%), 1,2,4,5-tetrakis(4-carboxyphenyl)-benzene ( $\geq 98\%$ ), 4,4'-azopyridine ( $\geq 98\%$ ), 1,2-di(pyridyl)ethylene ( $\geq 98\%$ ), 2,2'-bipyridine ( $\geq 98\%$ ), nitric acid ( $\geq 98\%$ ) and N,N-dimethylformamide (99%) have been purchased from Merck and used as received. All microcrystals have been synthesized as solvothermal following the procedure described below.

Synthesis of single crystals of  $[\text{Cd}_2(\text{TCPB})(\text{azopy})_{0.5}(\text{DMF})]$  **1**,  $[\text{Cd}_2(\text{TCPB})(\text{dpe})_{0.5}(\text{DMF})]$  **2**,  $[\text{Cd}_2(\text{TCPB})(\text{bipy})_2(\text{H}_2\text{O})]$  **3** (azopy - 4,4'-azopyridine, dpe - 1,2-di(pyridyl)ethylene, bipy - 2,2'-bipyridine) were carried out using similar established procedures. The mixture of compounds  $\text{Cd}(\text{NO}_3)_2 \cdot 4\text{H}_2\text{O}$  (24.67 mg, 0.08 mol),  $\text{H}_4\text{TCPB}$  (11.2 mg, 0.02 mol) and co-ligand (azopy 3.68 mg, 0.02 mol **1**; dpe 3.64 mg, 0.02 mol **2**; bipy 3.12 mg, 0.02 mol **3**) was dissolved in solvents 1.5 ml of N,N-dimethylformamide, 0.5 ml deionized water and 60  $\mu\text{l}$  nitric acid. The solution was placed in a 25 ml bottle and hermetically sealed with a lid with a rubber septum to prevent interaction with the external environment and create excess pressure in the vessel. The obtained solution was heated at 120 °C for 48 hours. The resulting single crystals were separated from the mother liquor by filtration, washed several times with N,N-dimethylformamide (2 ml) and EtOH (2 ml) and dried at 60°C for 12 hours. Yield =74% (45,5 mg) for **1**, 68% (41,2 mg) for **2** and 81% (50,7 mg) for **3**, as calculated for  $\text{H}_4\text{TCPB}$ .

### Characterizations.

#### SCXRD Analysis

CCDC for 2377923  $[\text{Cd}_2(\text{TCPB})(\text{azopy})_{0.5}(\text{DMF})]$  **1**, 2377924 for  $[\text{Cd}_2(\text{TCPB})(\text{dpe})_{0.5}(\text{DMF})]$  **2**, 2377925 for  $[\text{Cd}_2(\text{TCPB})(\text{bipy})_2(\text{H}_2\text{O})]$  **3**.

For single crystal X-ray analysis, a colorless crystal with dimensions of  $0.53 \times 0.10 \times 0.05$  mm **1**,  $0.42 \times 0.08 \times 0.08$  mm **2**,  $0.22 \times 0.07 \times 0.07$  mm **3**, was used. The unit cell parameters and the X-ray diffraction intensities were measured on Xcalibur Ruby diffractometer. The empirical absorption correction was introduced by multiscan method using SCALE3 ABSPACK algorithm. Using the Olex2, the structure was solved with the SHELXT program and refined by the fullmatrix least-squares method in the anisotropic approximation for all non-hydrogen atoms with the SHELXL program. Hydrogen atoms were positioned geometrically and refined using a riding model. The contribution of the solvent electron density was removed using the SQUEEZE routine in PLATON.

#### Powder X-ray diffraction

PXRD analysis has been performed using Bruker D2 PHASER diffractometer for vacuum-dried microcrystals (Göbel-mirror monochromated Cu  $K\alpha$  radiation  $\lambda=1.54056$  Å).

#### Scanning electron microscopy and elemental analysis

The SEM micrographs and element distribution have been obtained on FEI Quanta Inspect S (the basic scanning electron microscope (SEM) with Wcathode), occupied with Electron Probe X-ray Microanalysis Detector (SiLi 138 eV detector, SATW window) for elemental analysis.

#### Raman spectroscopy

Raman scattering has been analyzed under the excitation by a 632.8 nm continuous laser (He-Ne laser, Thorlabs) in reflection mode through 100x Mitutoyo M Plan Apo (NA = 0.9) objective. The collecting signal has been transferred to Horiba Labram monochromator occupied with 1800 g mm<sup>-1</sup> diffraction grating and water-cooling ANDOR CCD detector.

## Optical measurement

The experiment involved measuring the birefringence in metal-organic framework crystals by recording reflection and transmission spectra. The setup utilized a Glan prism mounted on a motorized rotator to adjust the polarization angle of unpolarized white light. Spectral data were collected over a range of wavelengths from 390 nm to 1000 nm, with a 10-degree step in the polarization angle. This method allowed for precise characterization of the optical anisotropy in MOF crystals, similar to approaches used in previous studies that investigated the unique anisotropic optical properties of MOF crystals composed of trinuclear iron(III) units linked by tetracarboxylic linkers [1]. Such MOFs often exhibit significant birefringence due to their structured composition, as demonstrated in studies where materials like  $[\text{RbSr}_3\text{X}][(\text{BS}_3)_2]$  ( $\text{X} = \text{Cl}, \text{Br}$ ) showed large birefringence values due to their unique structural arrangements [2].

## DFT calculations.

Periodic DFT calculations have been performed in CRYSTAL17 package [3] with BLYP functional and reduced atomic basis set [4]. Optimization of crystal structure with fixed cell parameters has been used for the obtaining of energy minimum with further analysis of Raman-active modes and their intensities accompanied by dynamic refractive indices calculation [5]. Selected wavelengths have been chosen in order to reproduce experimental procedure.

## Optical experiment.

Optical reflection measurement of metal-organic frameworks crystal at normal incidence was carried out to obtain refractive indices were performed on an experimental setup identical to [6]. For this experiment the confocal optical scheme

was arranged Figure S20. The incident unpolarized light from a halogen lamp (Avantes AVALIGHT-HAL-S-Mini) was focused on the crystal surface through a 100x microscope objective (Mitutoyo Plan APO NIR HR, NA 0.7). Glan-Taylor prisms (ThorLabs GT10) polarised this white light in the channels of reflectance and transmission. Reflected or transmitted light was collected through the same objective and then analyzed by a spectrometer (HORIBA LabRam HR) with a cooled CCD camera (Andor DU 420A-OE) and a 150 g/mm diffraction grating with a working window from 200 to 1100 nm. Due to the pinhole onto which the light was focused, the spectroscope became a confocal one. This allowed measuring the spectra from an area as small as  $4 \times 3 \mu\text{m}$ . The obtained spectra were normalized by the known spectrum of the halogen lamp. The reflectance spectra from different points of the crystal allowed us to estimate the error for refractive indices at various wavelengths.

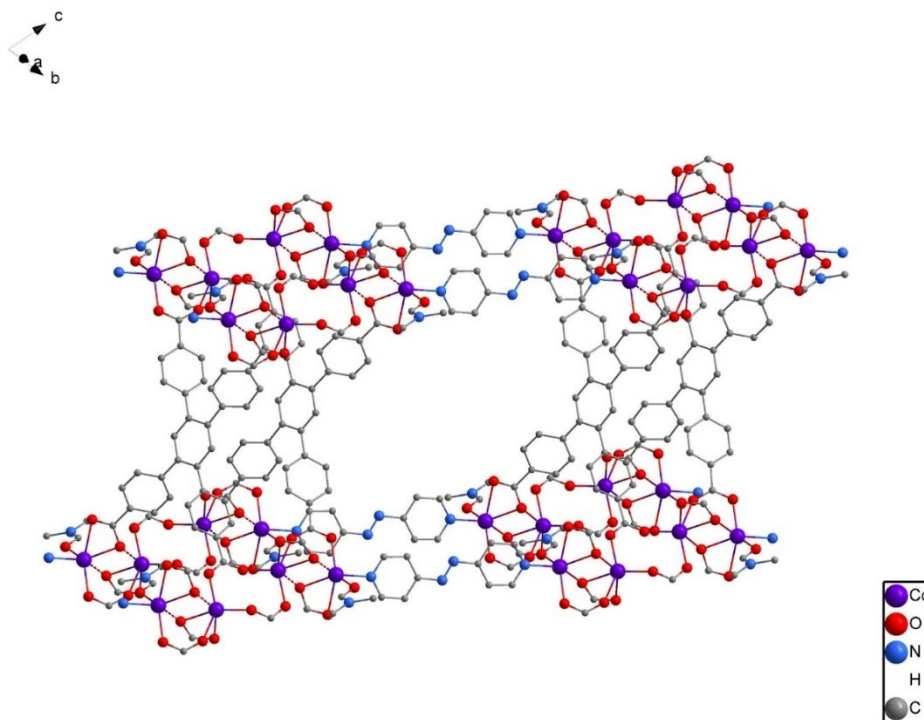


Figure S1. The crystal core view structure of  $[\text{Cd}_2(\text{TCPB})(\text{azopy})_{0.5}(\text{DMF})]$  **1**. The hydrogen atoms are omitted

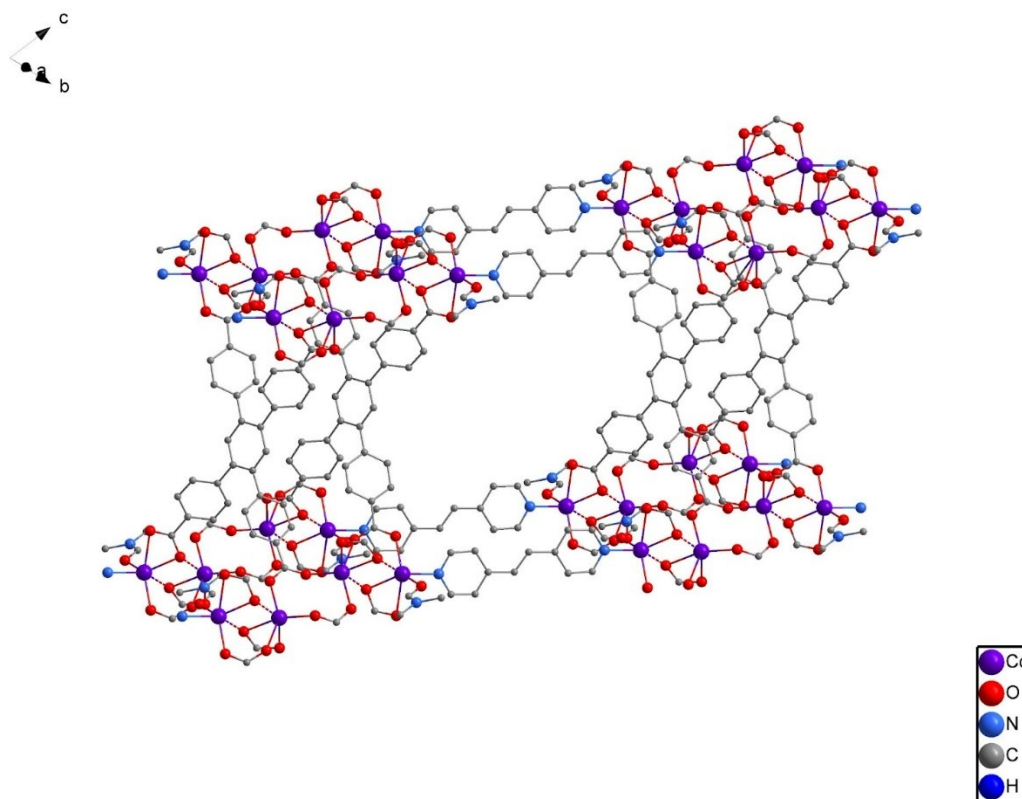


Figure S2. The crystal core view structure of  $[\text{Cd}_2(\text{TCPB})(\text{dpe})_{0.5}(\text{DMF})]$  **2**. The hydrogen atoms are omitted

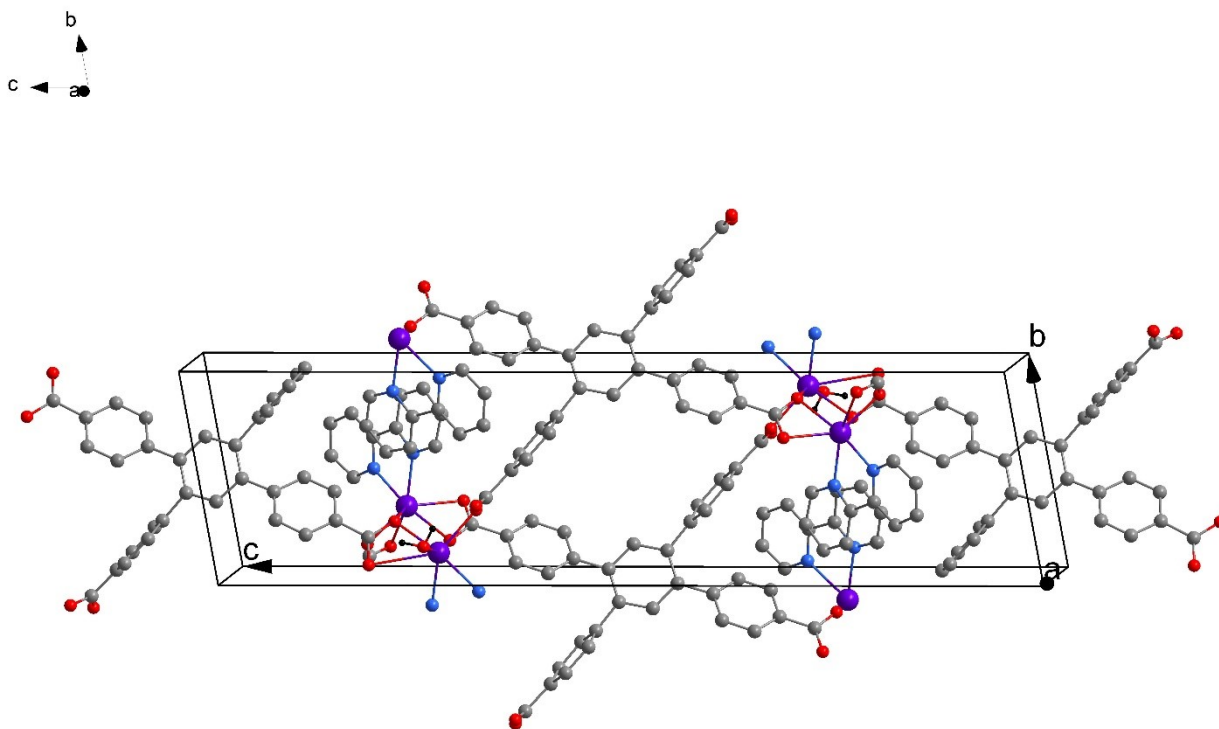


Figure S3. The crystal core view structure of  $[\text{Cd}_2(\text{TCPB})(\text{bipy})_2(\text{H}_2\text{O})]$  **3**. The hydrogen atoms are omitted (except water molecules).

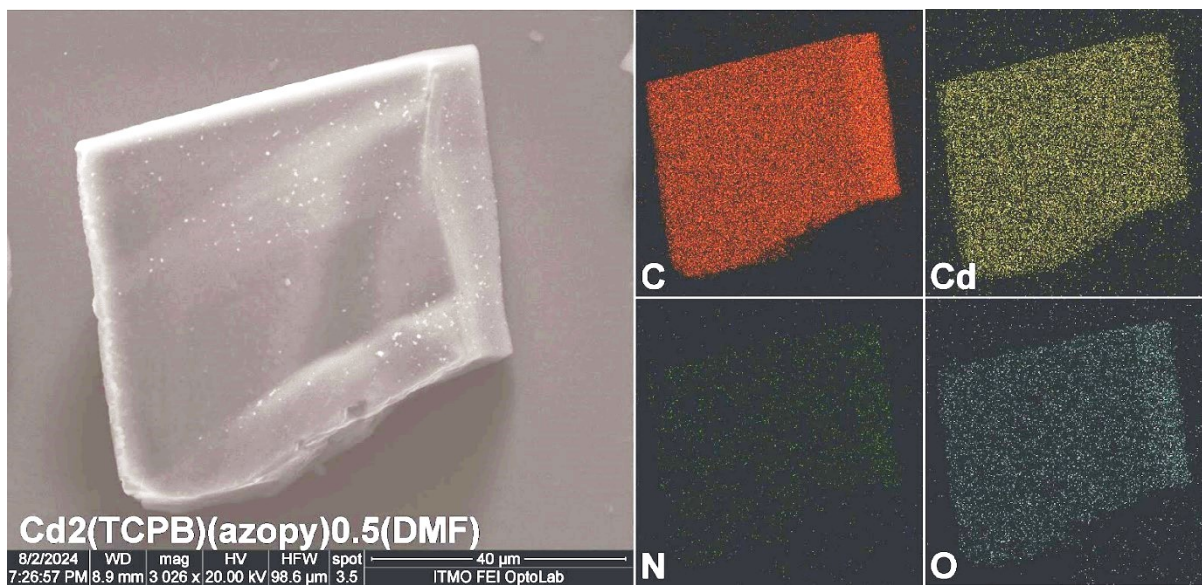


Figure S4. SEM-EDX analysis of  $[\text{Cd}_2(\text{TCPB})(\text{azopy})_{0.5}(\text{DMF})]$  **1**.

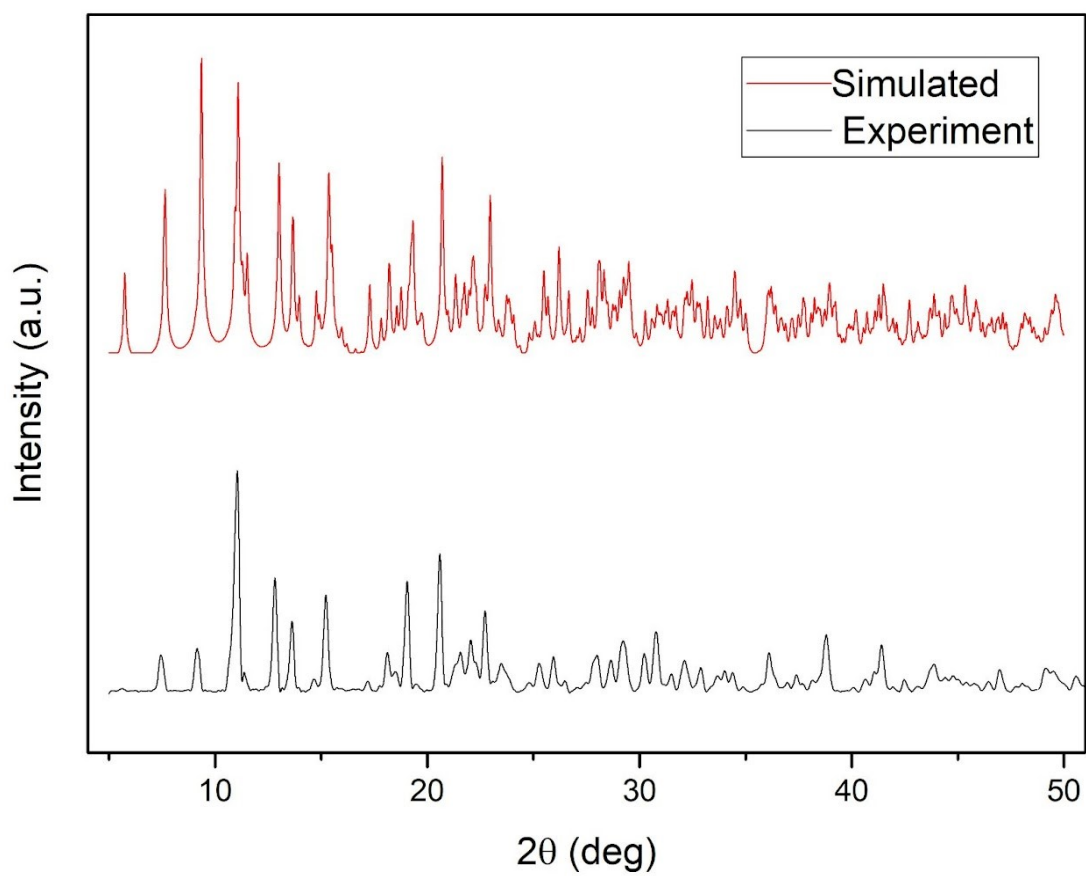


Figure S5. PXRD analysis of  $[\text{Cd}_2(\text{TCPB})(\text{azopy})_{0.5}(\text{DMF})]$  **1**.

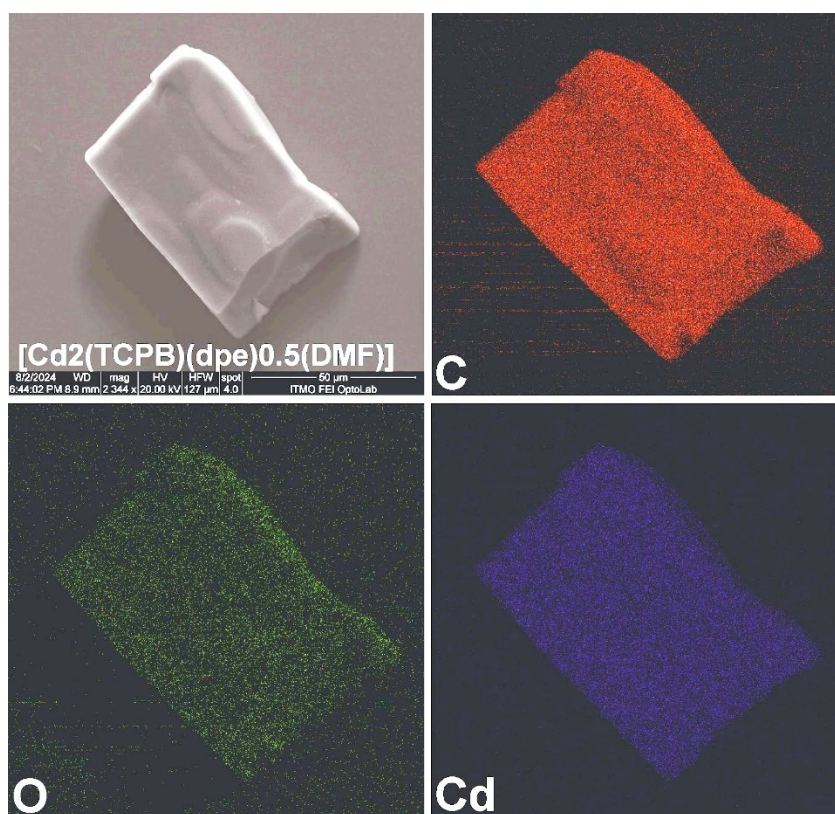


Figure S6. SEM-EDX analysis of  $[\text{Cd}_2(\text{TCPB})(\text{dpe})_{0.5}(\text{DMF})]$  **2**.

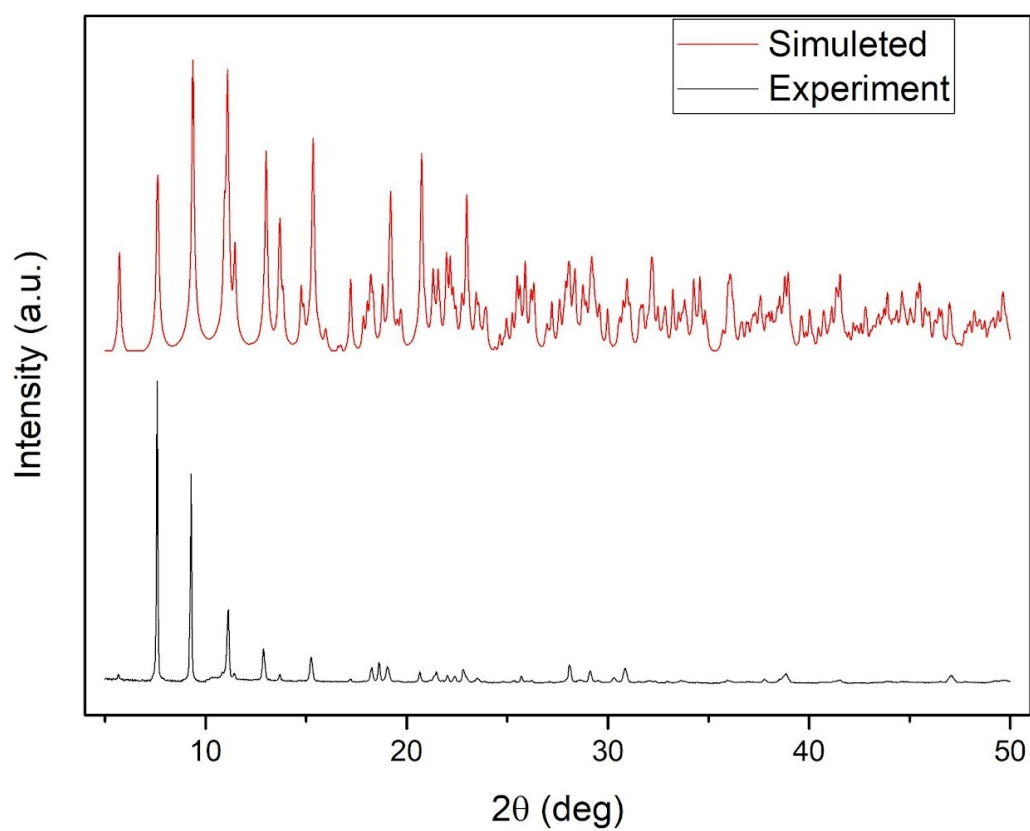


Figure S7. PXRD analysis of  $[\text{Cd}_2(\text{TCPB})(\text{dpe})_{0.5}(\text{DMF})]$  **2**.

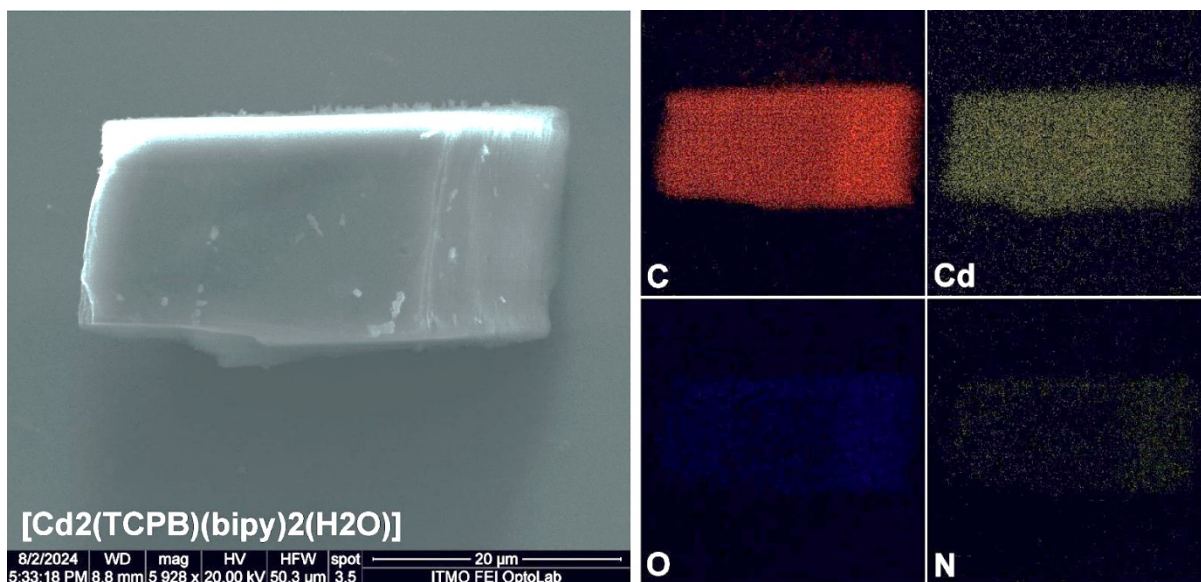


Figure S8. SEM-EDX analysis of  $[\text{Cd}_2(\text{TCPB})(\text{bipy})_2(\text{H}_2\text{O})]$  **3**.

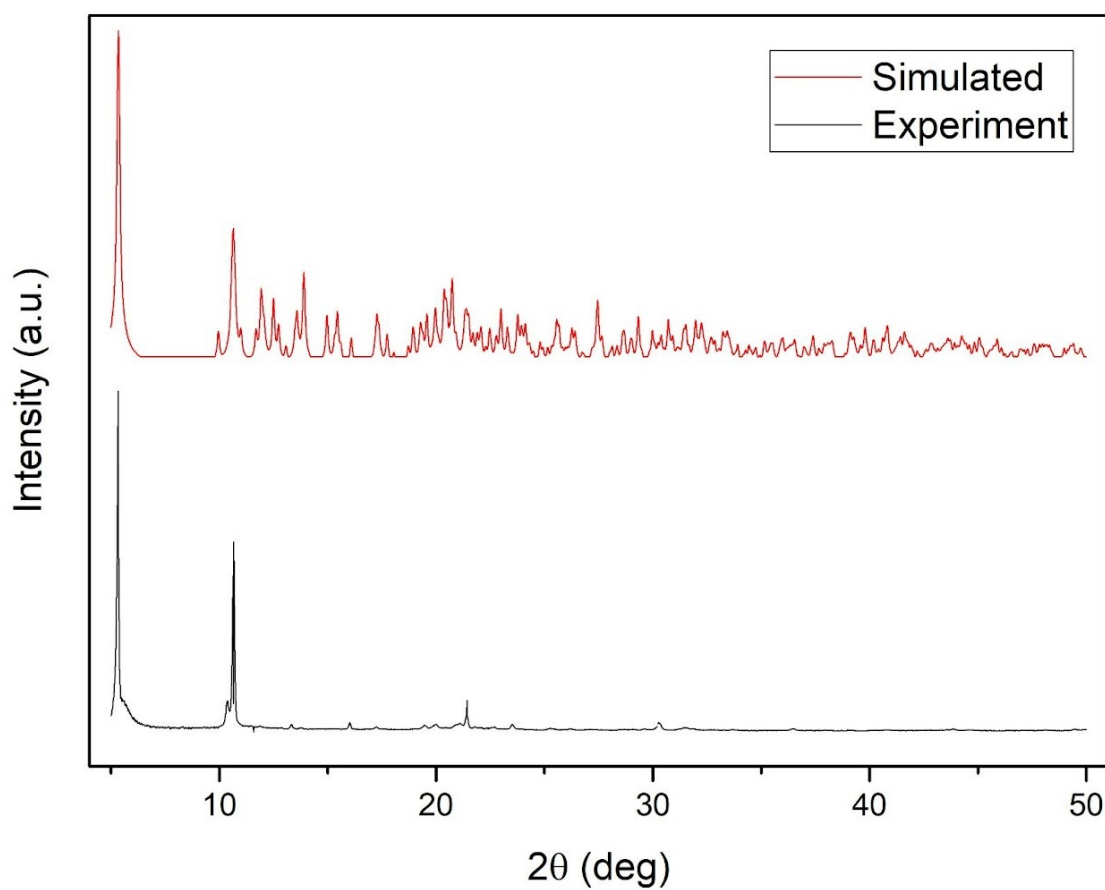


Figure S9. PXRD analysis of  $[\text{Cd}_2(\text{TCPB})(\text{bipy})_2(\text{H}_2\text{O})]$  **3**.

Table S1. Raman data and analysis of MOFs 1-3.

Wavenumber Range (cm <sup>-1</sup> )	Group	Intensity	Ref.
<b>[Cd<sub>2</sub>(TCPB)(azopy)<sub>0.5</sub>(DMF)] 1</b>			
109	Cd-O	strong	[7]
408	Cd-N	medium	[7]
853	C-O-C	medium	[8]
1009	C-C ring	medium	[7]
1157	C-C ring + C-H	strong	[7]
1231	C-H	medium	[7]
1317	C-C ring + C-H	strong	[7]
1410	C-N	medium	[9]
1459	N=N	strong	[7]
1525	C=C	medium	[7]
1603	C=O	strong	[7]
<b>[Cd<sub>2</sub>(TCPB)(dpe)<sub>0.5</sub>(DMF)] 2</b>			
109	Cd-O	strong	[7]
409	Cd-N	medium	[7]
857	C-O-C	medium	[8]
1014	C-C ring + C-H	medium	[7]
1199	C-H	medium	[7]
1316	C-C ring + C-H	strong	[7]
1419	C-N	medium	[7]
1533	C=C	medium	[7]
1607	C=O	strong	[7]
<b>[Cd<sub>2</sub>(TCPB)(bipy)<sub>2</sub>(H<sub>2</sub>O)] 3</b>			
91	Cd-O	strong	[7]
413	Cd-N	medium	[7]
857	C-O-C	medium	[8]
1018	C-C ring	medium	[7]
1143	C-C ring + C-H	strong	[7]
1230	C-H	medium	[7]
1312	C-C ring + C-H	strong	[7]
1414	C-N	medium	[7]
1529	C=C	medium	[7]
1603	C=O	strong	[7]

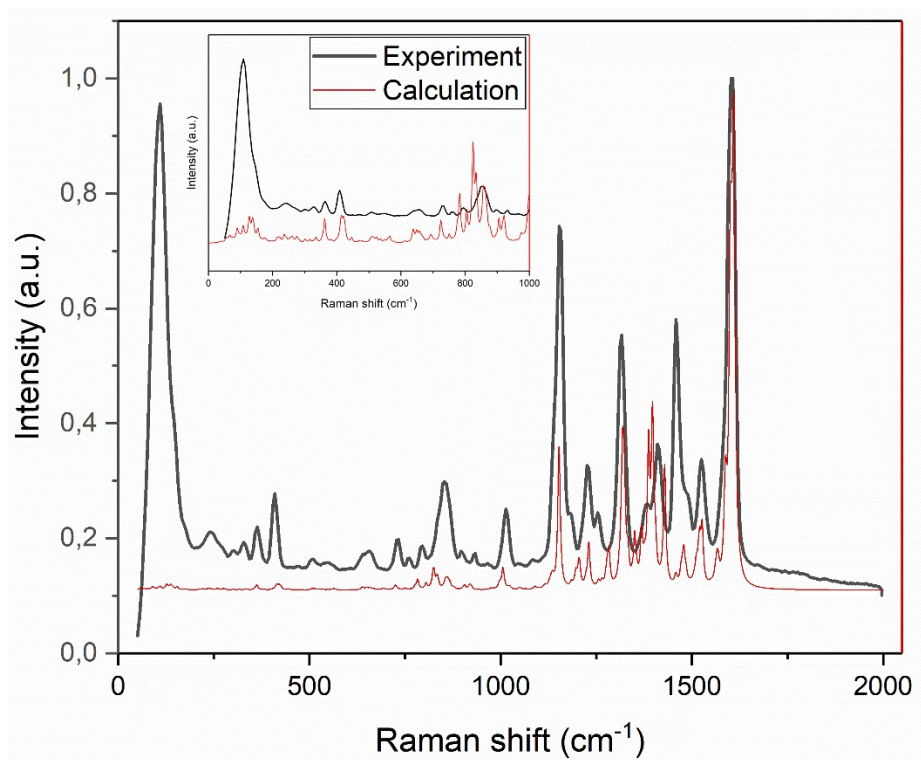


Figure S10. Calculated and experimental Raman spectra  
 $[\text{Cd}_2(\text{TCPB})(\text{azopy})_{0.5}(\text{DMF})]$  **1**.

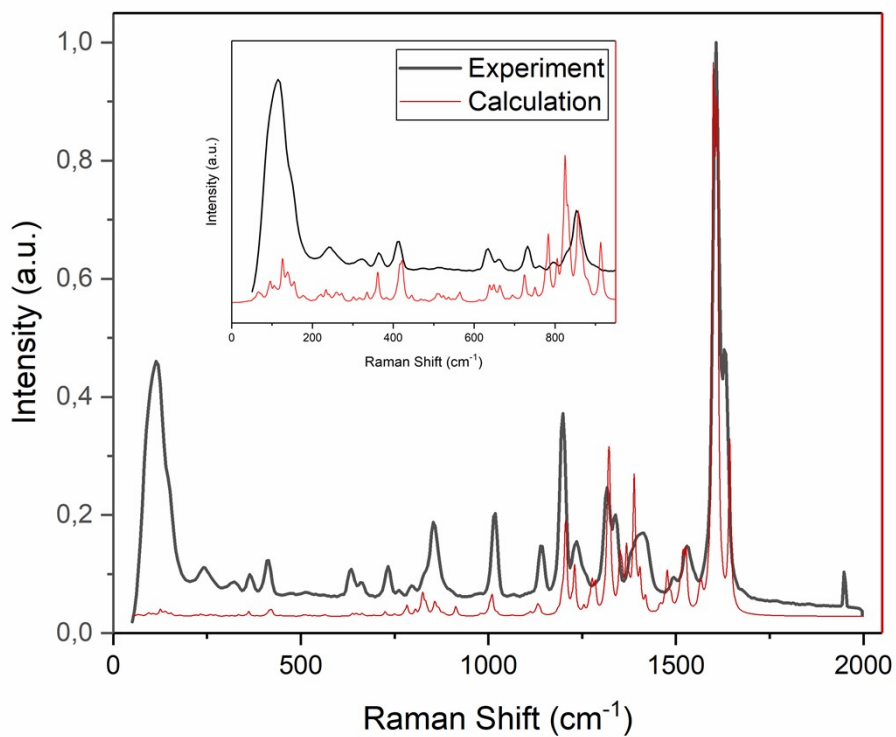


Figure S11. Calculated and experimental Raman spectra  
 $[\text{Cd}_2(\text{TCPB})(\text{dpe})_{0.5}(\text{DMF})]$  **2**.

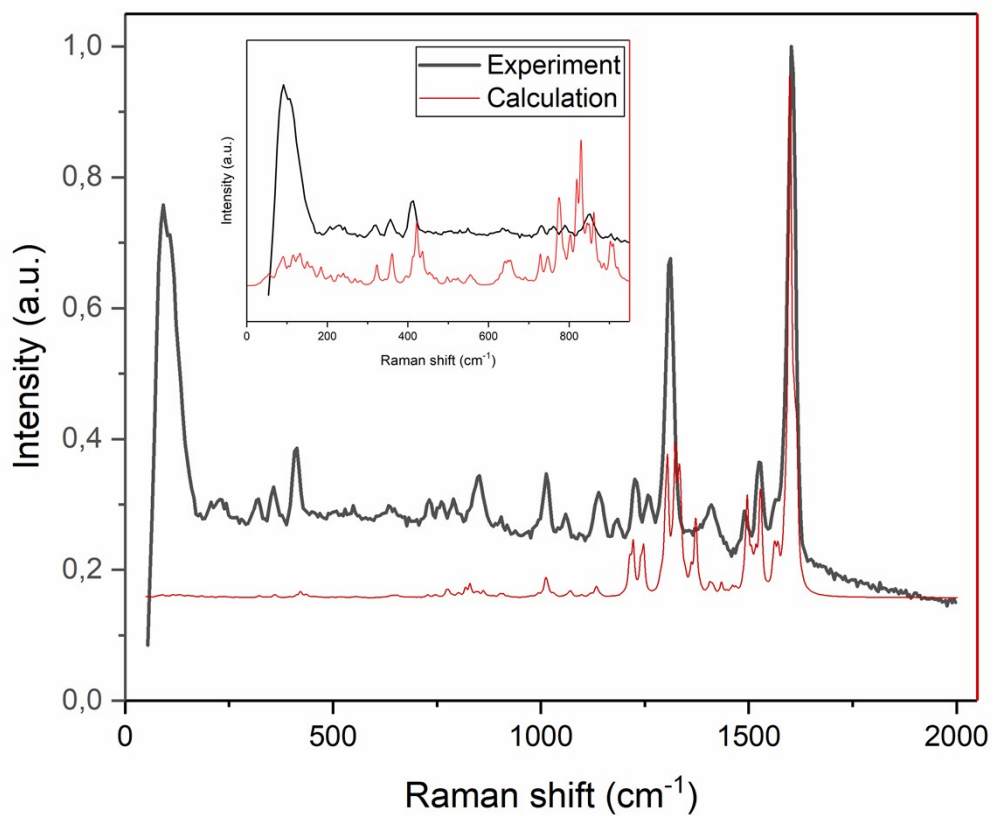


Figure S12. Calculated and experimental Raman spectra  
 $[\text{Cd}_2(\text{TCPB})(\text{bipy})_2(\text{H}_2\text{O})] \cdot 3$ .

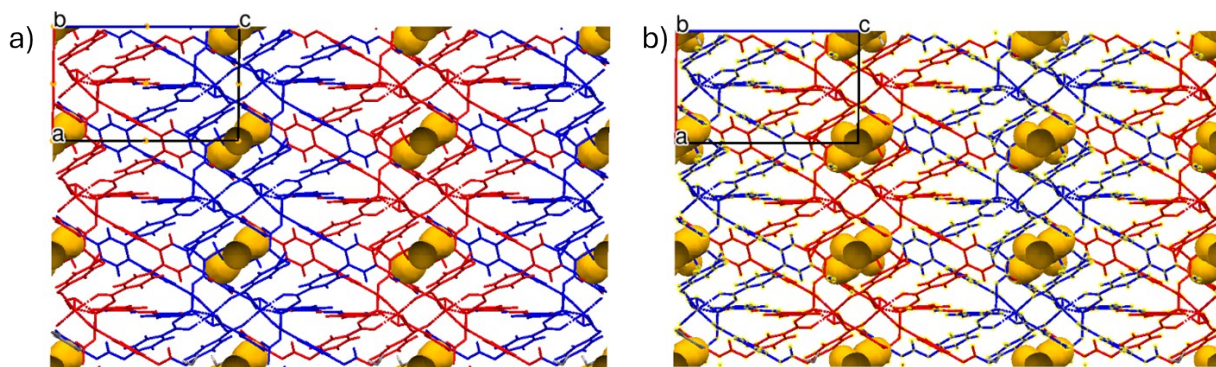


Figure S13. Fragments of crystal structure of MOFs **1** (a) and **2** (b) showing the voids (yellow spheres) and double interpenetration (the individual coordination nets are shown in red and blue)

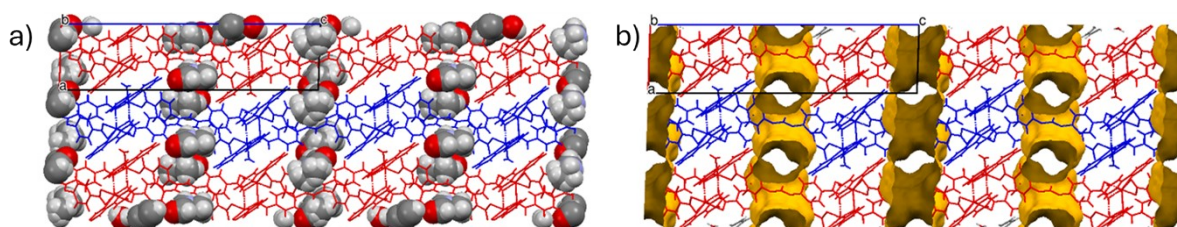


Figure S14. Fragments of crystal structure of MOF **3** showing the packing of 2D layers (the neighboring layers are shown in red and blue): (a) as-synthesized form with the voids filled with DMF molecules (shown as space-fill models); (b) hypothetical structure of **3** with removed DMF molecules showing two-dimensional channels (shown in yellow).

Table S2. Calculated porosity characteristics of MOFs **1-3**.

	<b>1</b>	<b>2</b>	<b>3</b>	<b>3 no DMF</b>
Void volume, % of cell	2.3	3.6	0	24.9
Network-accessible surface area per mass, m <sup>2</sup> /g	0	0	0	58.09
Network-accessible helium volume, cm <sup>3</sup> /g	0.011	0.012	0.001	0.218
Network-accessible geometric volume, cm <sup>3</sup> /g	0.169	0.174	0.171	0.279
Pore limiting diameter, Å	1.77	1.57	1.24	3.46
Maximum pore diameter, Å	2.5	2.57	2.02	4.9
Number of percolated dimensions	1	1	1	2

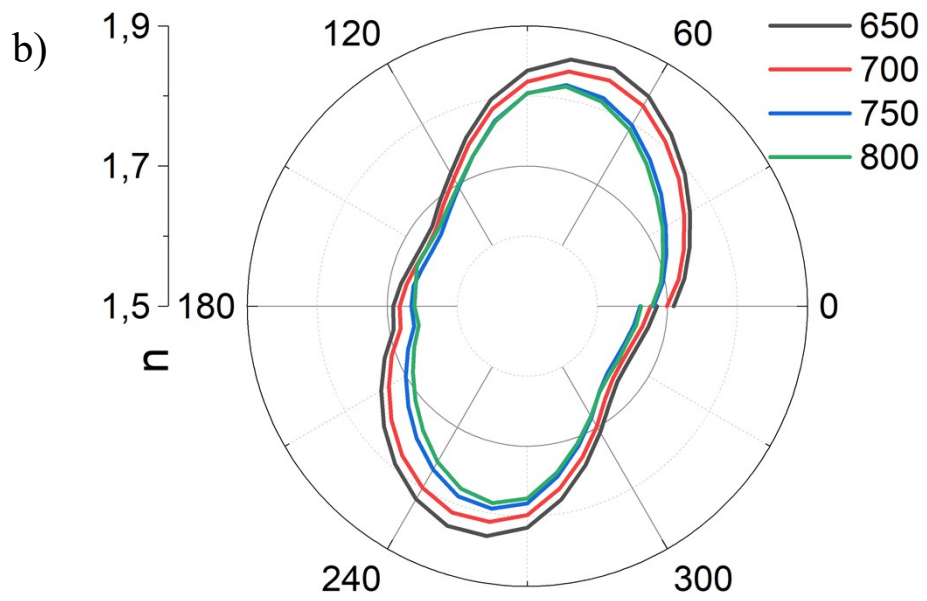
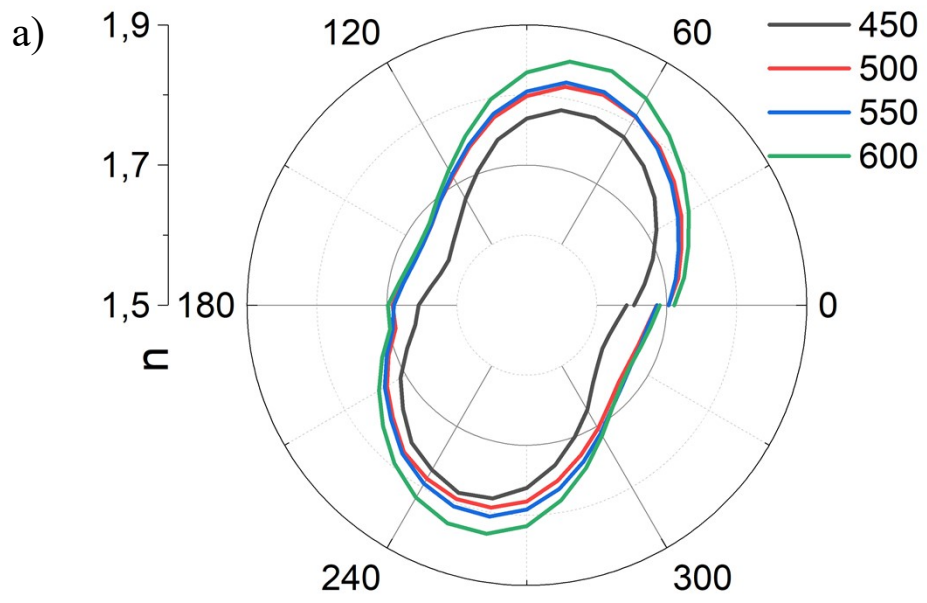
Table S3. Calculated dynamic refractive indices of the samples **1-3** at specified wavelengths chosen to reproduce experimental protocols.

	Sample					
	<b>1</b>		<b>2</b>		<b>3</b>	
Wavelength, nm	565	645	510	730	465	670
$n_1$	1.497	1.493	1.525	1.475	1.550	1.546
$n_2$	1.825	1.778	1.841	1.749	1.810	1.792
$n_3$	1.917	1.874	1.968	1.843	2.130	2.119
$n_{av}$	1.746	1.715	1.778	1.689	1.830	1.819
$\Delta n_1=n_2-n_1$	0.328	0.285	0.316	0.274	0.26	0.246
$\Delta n_2=n_3-n_1$	<b>0.42</b>	<b>0.381</b>	<b>0.443</b>	<b>0.368</b>	<b>0.58</b>	<b>0.573</b>
$\Delta n_3=n_3-n_2$	0.092	0.096	0.127	0.094	0.32	0.327

Periodic DFT calculations allowed correct ranging of the samples according to the increase in maximum value  $n_3$  and  $\Delta n$  so that the highest values are observed for the sample **3**. Unlike crystal **1** and **2**, in the crystal structure of **3** the pores on the framework are not empty: there are two symmetrically independent solvent molecules, one of which contains disordered atoms. It is worth noting that in quantum-chemical modelling we took into account both of them as it has been shown that empty network resulted in lowered values of calculated dynamic  $n$  values compared to the filled framework proving the consideration that solvent molecules in pores not only increase crystallographic density of the sample **3** but also impact refraction ability and polarizability of the studied crystal. Also, it has been found that in calculation frequency dependence mostly impacts on the  $n_3$  value with the maximum near below 500 nm which is in agreement with the experiment.

Table S4. Selected calculated tensor elements of dynamic polarizability tensor  $\alpha_{xx}$ ,  $\alpha_{yy}$  and  $\alpha_{zz}$  (a.u.) of the samples **2** and **3** (with or without solvent molecules) at 500 nm wavelength as a standard for the comparison.

500 nm	<b>3</b> with both solvent molecules	<b>3</b> without solvent molecules	<b>2</b>
$\alpha_{xx}$	2212	1936	1617
$\alpha_{yy}$	2505	2153	2143
$\alpha_{zz}$	3825	3427	2815



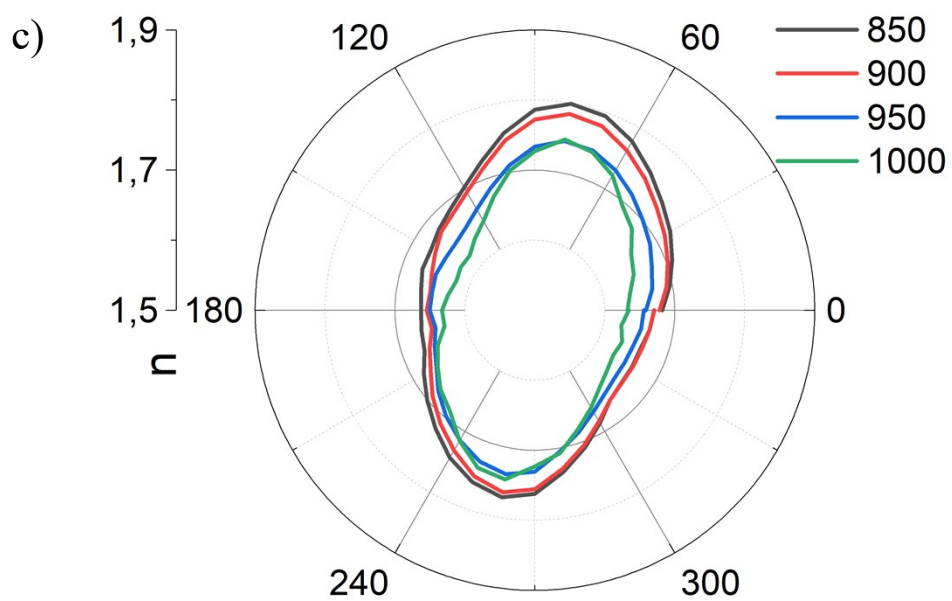
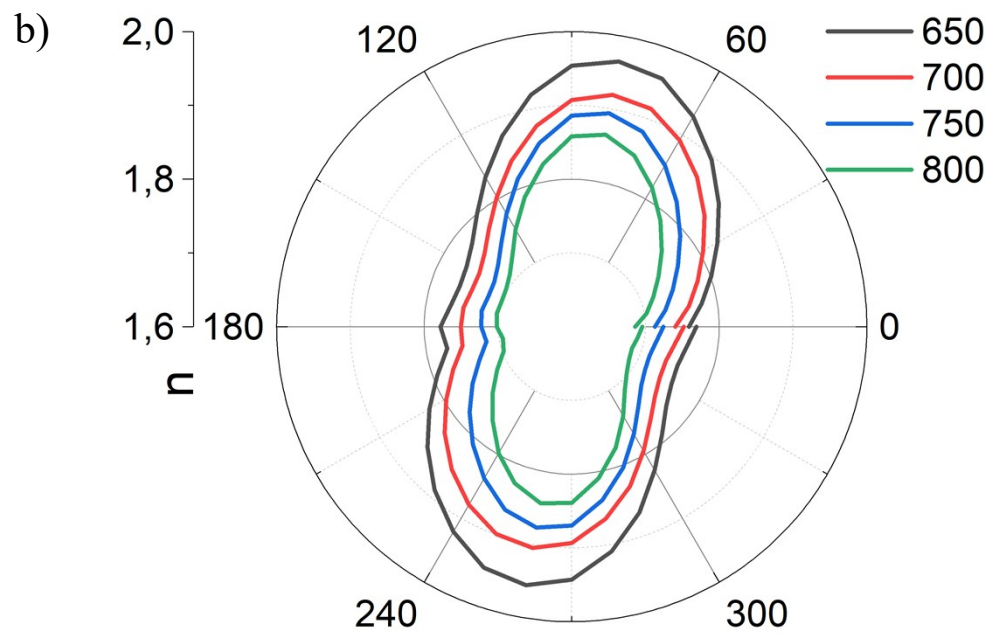
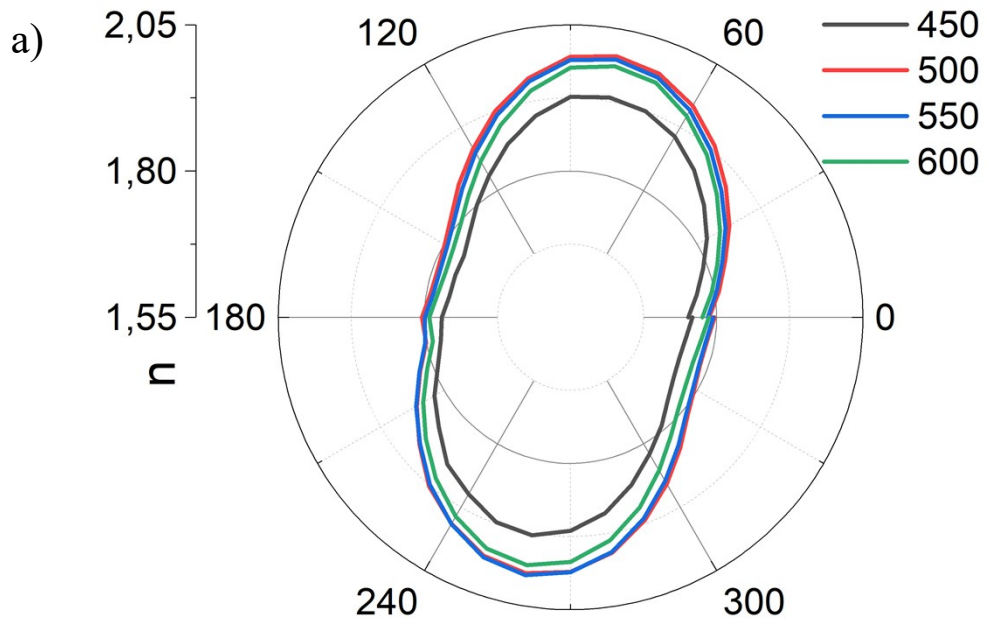


Figure S15. Polarization diagrams  $n$  for different spectral range a) 400-600, b) 600-800 and c) 800-1000 nm for  $[\text{Cd}_2(\text{TCPB})(\text{azopy})_{0.5}(\text{DMF})] \mathbf{1}$ .



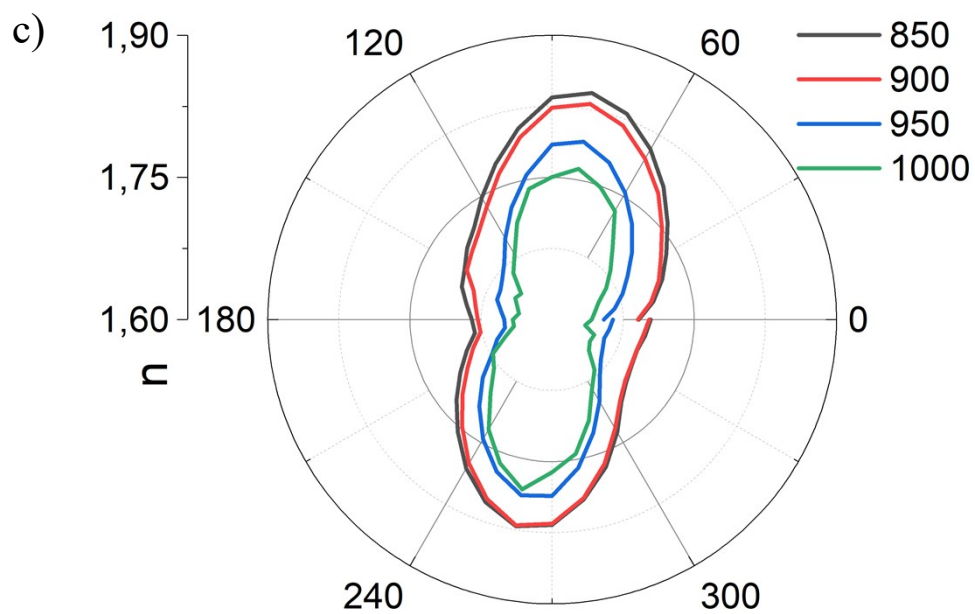
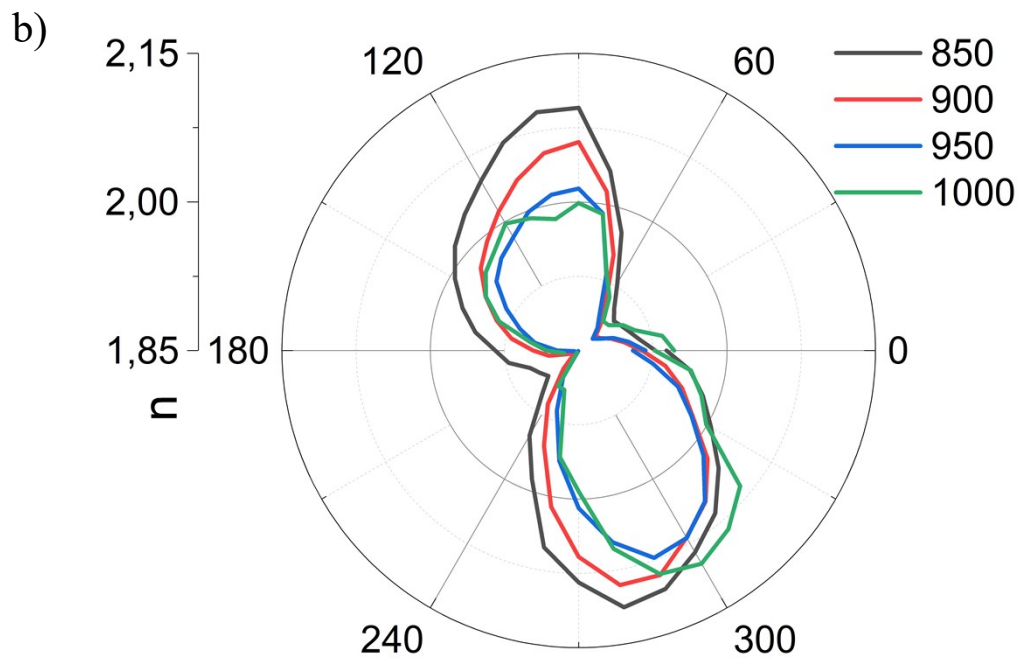
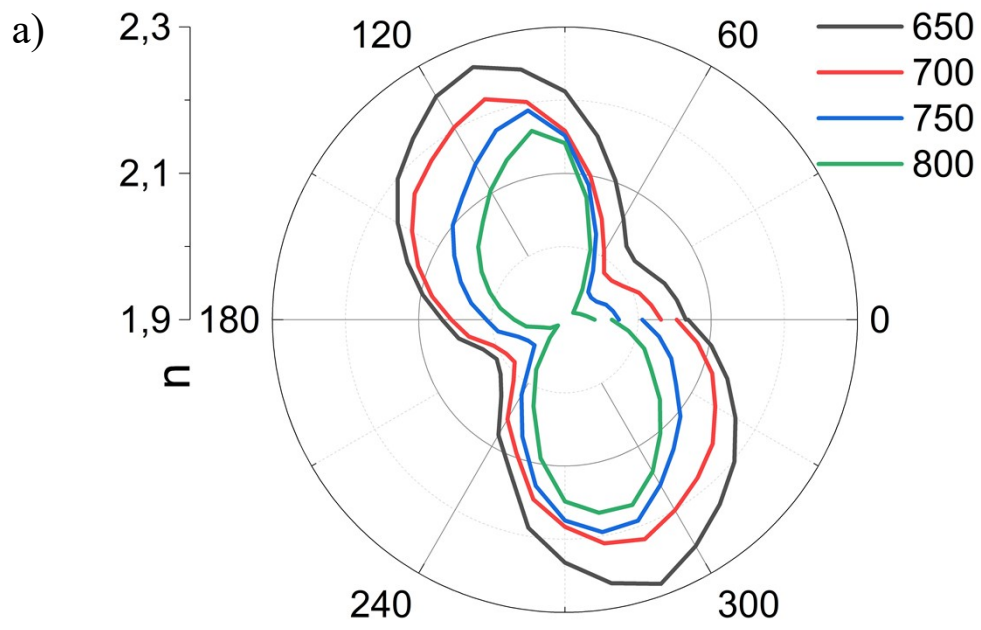


Figure S16. Polarization diagrams  $n$  for different spectral range a) 400-600, b) 600-800 and c) 800-1000 nm for  $[\text{Cd}_2(\text{TCPB})(\text{dpe})_{0.5}(\text{DMF})] \mathbf{2}$ .



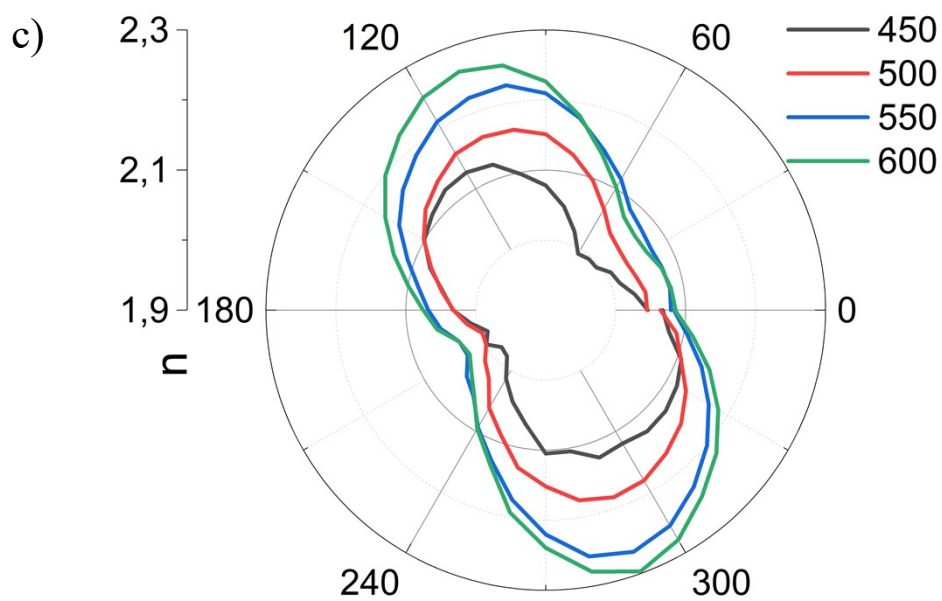


Figure S17. Polarization diagrams  $n$  for different spectral range a) 400-600, b) 600-800 and c) 800-1000 nm for  $[\text{Cd}_2(\text{TCPB})(\text{bipy})_2(\text{H}_2\text{O})]$  **3**.

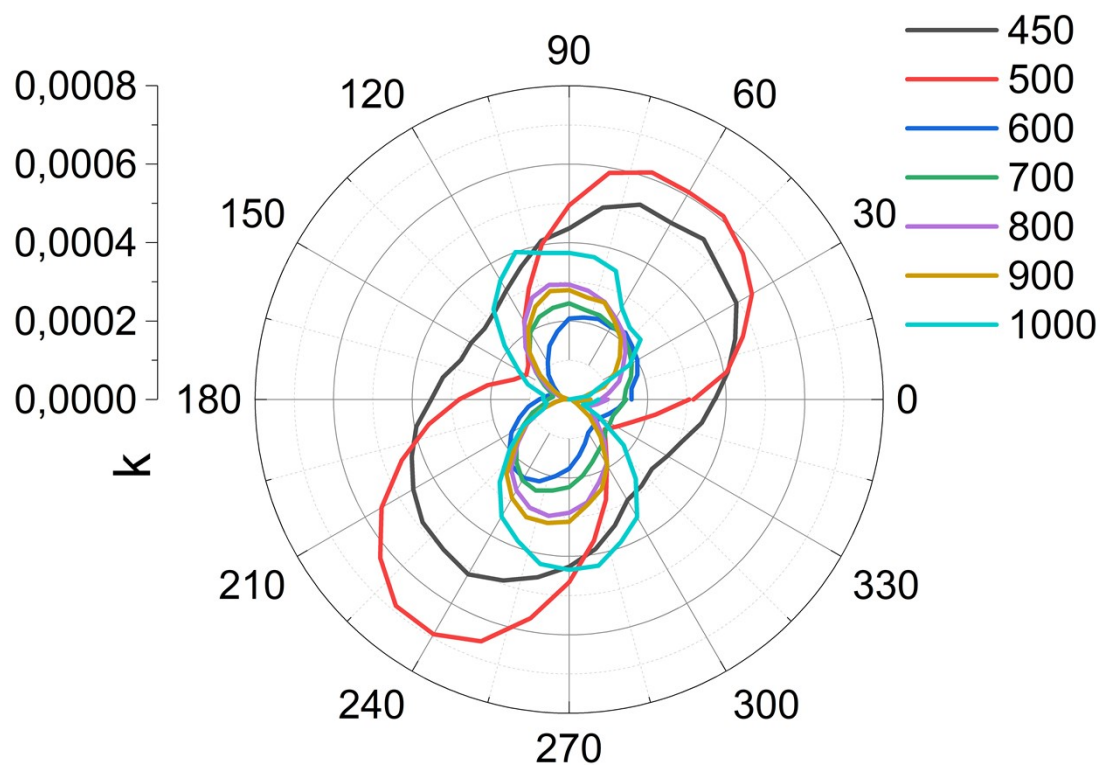


Figure S18. Polarization diagrams  $k$  [ $\text{Cd}_2(\text{TCPB})(\text{azopy})_{0.5}(\text{DMF})$ ] **1**.

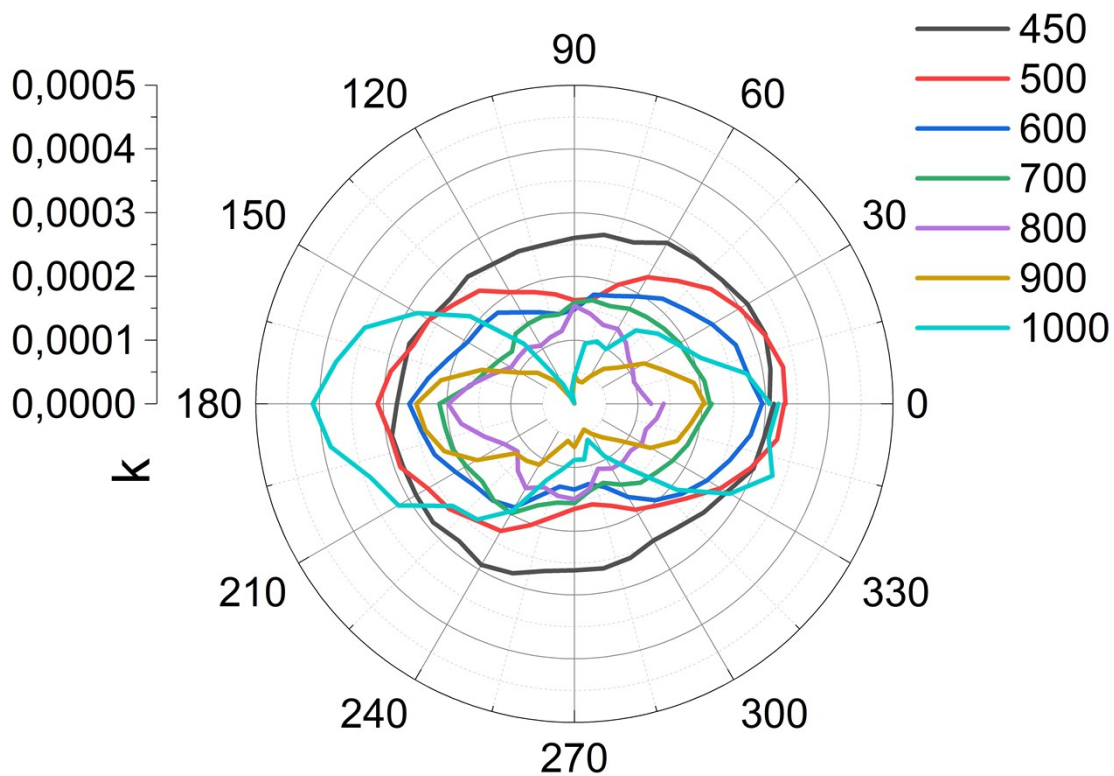


Figure S19. Polarization diagrams  $k$  [ $\text{Cd}_2(\text{TCPB})(\text{dpe})_{0.5}(\text{DMF})$ ] **2**.

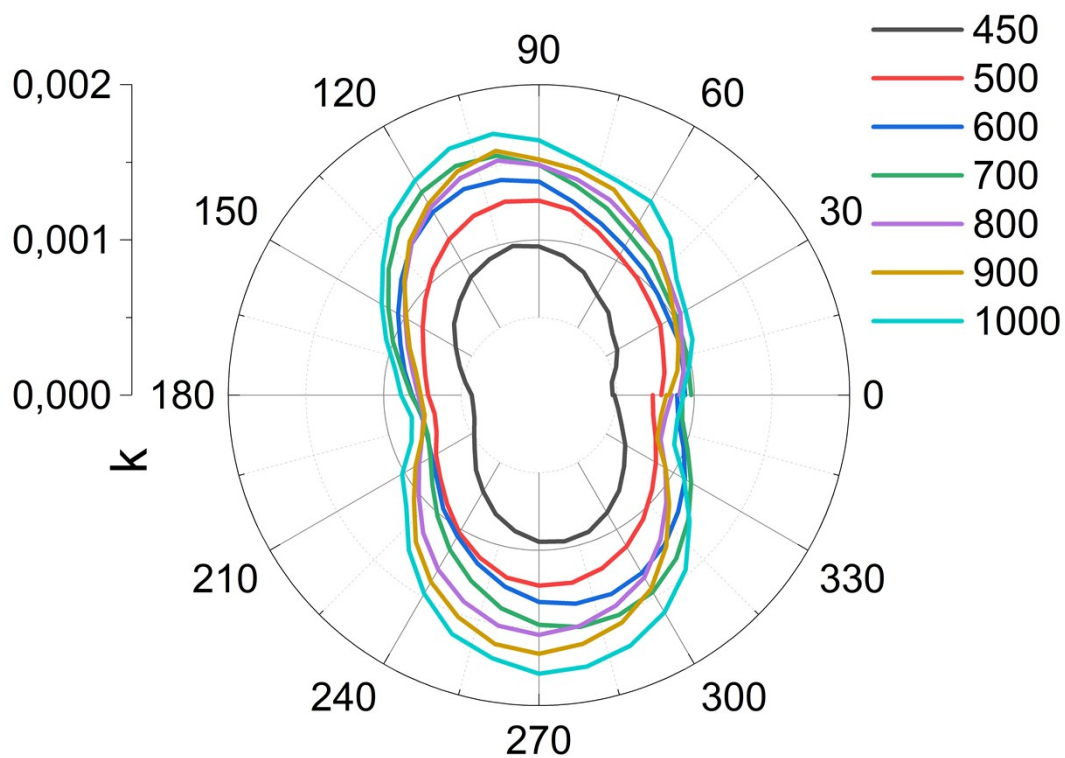


Figure S20. Polarization diagrams  $k$  [ $\text{Cd}_2(\text{TCPB})(\text{bipy})_2(\text{H}_2\text{O})$ ] **3**.

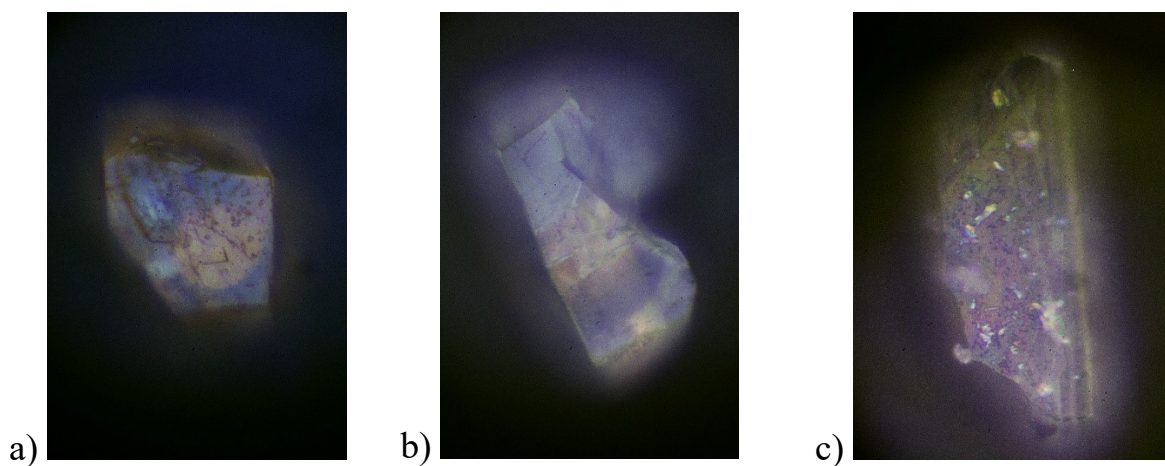


Figure S21. Samples photo before experiment: a) – **1**, b) – **2**, c) – **3**.

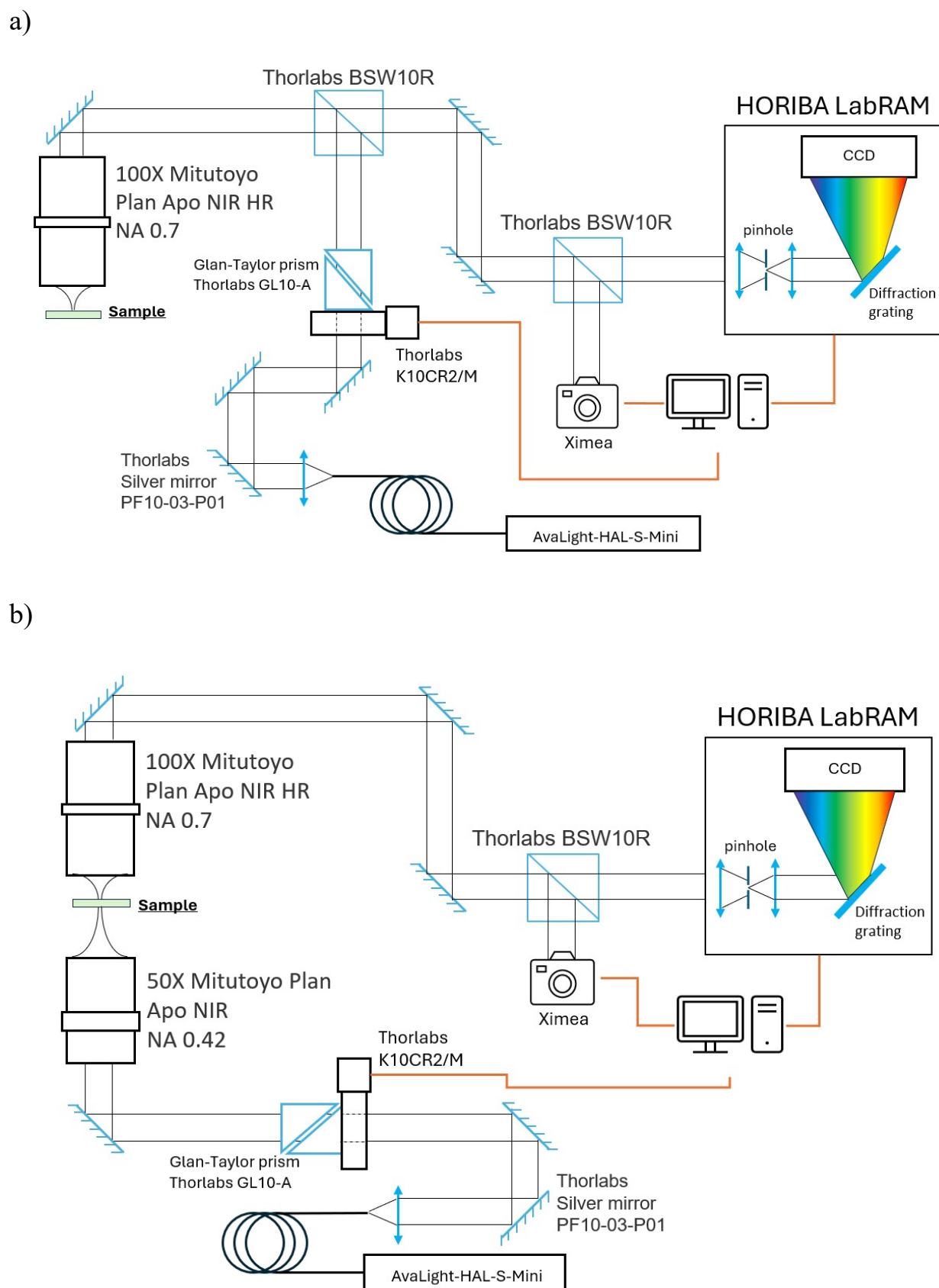


Figure S22. Experimental setup a) Reflectance measurement; b) Transmittance measurement.

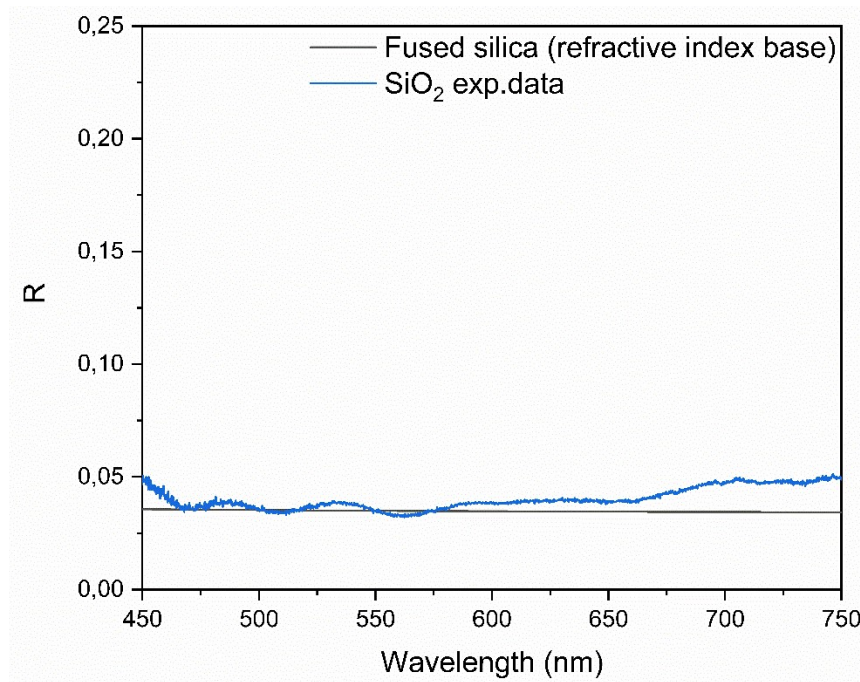


Figure S23. The reflection spectrum of the glass substrate obtained during the experiment in comparison with the reference spectrum of amorphous silica [10].

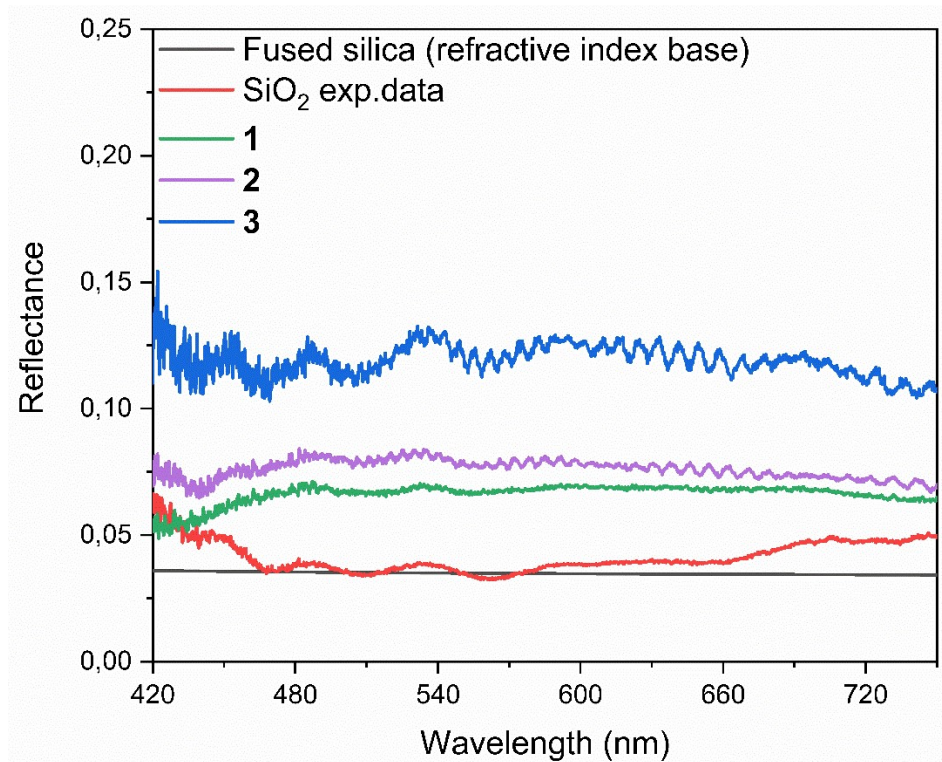


Figure S24. The reflection spectra of crystals **1**, **2**, **3**, the substrate, and the reference spectrum of glass. The interference features of the spectra (maxima in the substrate spectrum and minima in the crystal spectra) indicate that the substrate has a minimal effect on the reflection spectra of the crystals.

Table S5. Crystal data and structure refinement for **1-3**.

Identification code	[Cd <sub>2</sub> (TCPB)(azopy) <sub>0.5</sub> (DMF)] <b>1</b>	[Cd <sub>2</sub> (TCPB)(dpe) <sub>0.5</sub> (DMF)] <b>2</b>	[Cd <sub>2</sub> (TCPB)(bipy) <sub>2</sub> (H <sub>2</sub> O)] <b>3</b>
Empirical formula	C42H29Cd2N3O9	C43H30Cd2N2O9	C54H36Cd2N4O9
Formula weight	944,48	943.49	1255.86
Temperature, K	150,00	150,00	150,00
Crystal size, mm	0.53 × 0.10 × 0.05	0.42 × 0.08 × 0.08	0.22 × 0.07 × 0.07
Crystal system	triclinic	triclinic	triclinic
Space group	P-1 (2)	P-1 (2)	P-1 (2)
a, Å	9.5832(8)	9.5713(7)	8.8208(4)
b, Å	12.5689(10)	12.6619(8)	9.4521(6)
c, Å	16.4854(13)	16.6423(9)	33.3336(17)
α, deg	68.806(3)°	68.088(2)	82.639(2)
β, deg	87.073(3)°	86.824(2)	89.466(2)
γ, deg	80.317(3)°	80.224(2)	71.506(2)
V, Å <sup>3</sup>	1824.89(26)	1844.0(2)	2612.5(2)
Density (calc.), g/cm <sup>-3</sup>	1.719	1.699	1.596
Absorption coefficient, mm <sup>-1</sup>	1.229	1.215	0.885
F(000)	940	940	1272
Theta range, deg.	1.761 - 27.151	1.764 - 27.150	1.849 - 26.414
Index ranges	-12 ≤ h ≤ 12 -16 ≤ k ≤ 16 -21 ≤ l ≤ 21	-12 ≤ h ≤ 12 -16 ≤ k ≤ 16 -21 ≤ l ≤ 21	-11 ≤ h ≤ 11 -11 ≤ k ≤ 11 -41 ≤ l ≤ 41
Reflections	8048	8127	10678

collected			
Independent reflections, R <sub>int</sub>	5679 [R(int) = 0.0456]	5831 [R(int) = 0.0474]	7703 [R(int) = 0.0431]
Parameters refined	508	508	693
Goodness-of-fit on F <sup>2</sup>	0.986	1.028	1.060
R1 / wR2 for I > 2σ(I)	R1 = 0.0456, wR2 = 0.0547	R1 = 0.0474, wR2 = 0.0507	R1 = 0.0531, wR2 = 0.0505
R1 / wR2 for all data	R1 = 0.0768, wR2 = 0.0860	R1 = 0.077, wR2 = 0.0991	R1 = 0.0763, wR2 = 0.1084
Extinction coefficient	0.00044(15)	0.00031(16)	0.0012(3)
T <sub>max</sub> , T <sub>min</sub>	0.7455, 0.6306	0.7455, 0.6490	0.7454, 0.6811
Δρ <sub>max</sub> / Δρ <sub>min</sub> , e.Å <sup>-3</sup>	0.609 / -0.836	0.893 / -0.994	2.324 / -0.742

Table S6: Main structural parameters for **1-3**.

MOF	Cd-O, distance, Å	Cd-N, distance, Å	Cd-Cd distance in core, Å
<b>1</b>	Cd-O(TCBP) = 2.30 - 2.42 Å Cd-O(DMF) = 2.25 Å	Cd-N(azopy) = 2.31 Å	Cd-Cd = 3.34 Å
<b>2</b>	Cd-O(TCBP) = 2.31 - 2.42 Å Cd-O(DMF) = 2.25 Å	Cd-N(dpe) = 2.28 Å	Cd-Cd = 3.42 Å
<b>3</b>	Cd-O(TCBP) = 2.32 - 2.75 Å, Cd-O(H <sub>2</sub> O) = 2.28 Å	Cd-N(bipy) = 2.28 - 2.40	Cd-Cd = 3.82 Å

**Reference**

- [1] I. Chi-Durán, R. A. Fritz, R. Urzúa-Leiva, G. Cárdenas-Jirón, D. Pratap Singh, F. Herrera, *ACS Omega*, **2022**, 7, 28, 24432–24437.
- [2] Y. Yihan, H. Xueling, Y. Zhihua, L. Guangmao, P. Shilie, *Chem. Commun.*, **2024**, 60, 118-121.
- [3] R. Dovesi, A. Erba, R. Orlando, C. M. Zicovich-Wilson, B. Civalleri, L. Maschio, M. Rerat, S. Casassa, J. Baima, S. Salustro, B. Kirtman. *WIREs Comput Mol Sci.*, **2018**, 8, e1360.
- [4] a) C. Gatti, V.R. Saunders, C. Roetti, "Crystal-field effects on the topological properties of the electron-density in molecular-crystals - the case of urea", *J. Chem. Phys.*, **1994**, 101, 10686-10696; b) M.A. Spackman, A.S. Mitchell, "Basis set choice and basis set superposition error (BSSE) in periodic Hartree-Fock calculations on molecular crystals", *Phys. Chem. Chem. Phys.*, **2001**, 3, 1518-1523.
- [5] a) L. Maschio, B. Kirtman, M. Rerat, R. Orlando and R. Dovesi, *J. Chem. Phys.*, **2013**, 139, 164101; b) M. Ferrero, M. Rerat, R. Orlando, R. Dovesi, *J. Comput. Chem.*, **2008**, 29, 1450.
- [6] A. V. Vinogradov, V. A. Milichko, H. Zaake-Hertling, A. Aleksovskaya, S. Gruschinski, S. Schmorl, B. Kersting, E. M. Zolnhofer, J. Sutter, K. Meyer, P. Lönnecke and E. Hey-Hawkins, *Dalton Trans.*, **2016**, 45, 7244-7249.
- [7] H.C. Garcia, R. Diniz, M.I. Yoshida, L.F.C. de Oliveira, *CrystEngComm*, **2009**, 11, 881-888.
- [8] [https://static.horiba.com/fileadmin/Horiba/Technology/Measurement\\_Techniques/Molecular\\_Spectroscopy/Raman\\_Spectroscopy/Raman\\_Academy/Raman\\_Tutorial/Raman\\_bands.pdf?utm\\_source=uhw&utm\\_medium=301&utm\\_campaign=uhw-redirect](https://static.horiba.com/fileadmin/Horiba/Technology/Measurement_Techniques/Molecular_Spectroscopy/Raman_Spectroscopy/Raman_Academy/Raman_Tutorial/Raman_bands.pdf?utm_source=uhw&utm_medium=301&utm_campaign=uhw-redirect)
- [9] <https://www.chem.uci.edu/~dmitryf/manuals/Raman%20correlations.pdf>
- [10] I. H. Malitson, Interspecimen comparison of the refractive index of fused silica, *J. Opt. Soc. Am*, 1965, **55**, 1205-1208.
- [11] A.V. Yakovlev, V.A. Milichko, V.V. Vinogradov, A.V. Vinogradov, *ACS Nano.*, 2016, **10**, 3078-3086.